R. & M. No. 3565

MINISTRY OF TECHNOLOGY

AERONAUTICAL RESEARCH COUNCIL
REPORTS AND MEMORANDA

Boundary-Layer Interaction Effects in Intakes with Particular Reference to those Designed for Dual Subsonic and Supersonic Performance

By J. SEDDON, Ph.D.

LONDON: HER MAJESTY'S STATIONERY OFFICE
1970
PRICE 13*s* 0*d* [65*p*] NET

Boundary-Layer Interaction Effects in Intakes with Particular Reference to those Designed for Dual Subsonic and Supersonic Performance

By J. SEDDON, Ph.D.

Reports and Memoranda No. 3565*
March, 1966

Summary.

The nature of flow in intakes with external boundary layer, at subsonic and supersonic speeds, is described. On the basis of a systematic series of wind-tunnel tests, a quantitative assessment is made of the loss or pressure recovery due to interaction between the boundary layer and the pre-entry pressure gradient, including the normal shock when present. The analysis leads to a formula which is suggested for general application.

Boundary-layer control to reduce or eliminate the interaction loss may require to take special form when it is necessary not only to safeguard the supersonic performance but also to minimise the subsonic drag. Some brief discussion of this problem is given.

LIST OF CONTENTS

*Replaces R.A.E. Tech. Report No. 66 099—A.R.C. 28 368.

---

1. *Introduction.*

The pre-entry flow field of an air-intake in high speed flight is characterised in nearly all cases by a sharp rise in pressure. On subsonic aircraft the pressure rise is that associated with a spillage of air corresponding to the design entry flow ratio of the intake

$$A_\infty/A_i = \rho_i V_i/\rho_\infty V_\infty$$

being less than unity. On supersonic aircraft the pressure rise corresponds to the deceleration of air through a shock-wave system, which may or may not be followed by a further (subsonic) deceleration before the entry.

In the case of true pitot intakes for subsonic and possibly low supersonic speeds (e.g. with podded engines), the pre-entry pressure rise poses no particular problem in relation to design for good pressure recovery and flow distribution. In all other cases (on subsonic aircraft fuselage side intakes, wing-root intakes, intakes in swept leading edges etc; and on supersonic aircraft all intakes with external compression surfaces, whatever their location) the pre-entry pressure rise has an important influence on the design, on account of its interaction with boundary layers in the flow field approaching the entry plane.

Basically the nature of the interaction is that the pre-entry pressure rise can cause distortion of the boundary-layer profile and in many cases flow separation. The results on pressure recovery and flow distribution in the intake are almost always adverse. Because of this it has become the accepted practice in many situations to avoid, or at least minimise, the interaction effect by use of a boundary-layer bleed or diverter. To the extent to which the boundary layer is thereby by-passed from the main intake, the viscous interaction effects are eliminated and design values of pressure recovery, with correspondingly high levels of flow uniformity, are achieved.

In some circumstances, however, the use of a boundary-layer bleed or the equivalent cannot be accepted without challenge. Aspects such as the additional structural and mechanical complication and weight may rule it out, for example on ramjet intakes for supersonic missiles. On an aircraft where range capability is important, the drag associated with a bleed or diverter system must be considered, since this is capable of offsetting completely the gain accruing from increased pressure recovery.

A case in which the choice can be particularly difficult to make is that of a fuselage side intake on an aircraft designed for subsonic range performance coupled with a supersonic dash. For the subsonic cruise the main aerodynamic emphasis is likely to be on minimisation of the drag, to which end alone the bleed. or diverter arrangement would require to be itself minimised or even eliminated. Against this the bleed requirement for supersonic operation is likely *ab initio* to be considerably greater than that for subsonic, implying excessive drag if maintained down to the subsonic regime.

It is therefore both of fundamental interest and also of practical significance to study the nature of the viscous interaction in intakes with external boundary layer, at both subsonic and supersonic speeds. This is done in the present report, on the basis of a series of wind-tunnel experiments made with pitot-type

intakes mounted on a flat plate. The applicability of this arrangement is fairly general; for the boundary layer on the plate can be equated in practice with that on the fuselage of a side intake for subsonic and low supersonic speeds, or with that on the external compression surface (single-angle cone or wedge) of an intake for higher supersonic speeds. The tunnel Mach number corresponds in the former case to the flight speed (approximately); in the latter case to the Mach number on the compression surface ahead of the terminal shock. The range of tunnel Mach number covered in the tests was from 0·5 to 1·8.

Section 2 contains a description of the nature of the flow with viscous interaction and shows the order of magnitude of its effect on pressure recovery. In Section 3 quantitative assessments are made, based on the experimental results for a variety of shapes: leading to a generalised expression for the interaction loss, which is then checked against independent evidence obtained for realistic intake arrangements. Section 4 discusses the limitations and implications of the generalised result, leading to suggestions for future lines of experiment, either as general research or in the development of specific intakes.

2. *The Flow in Intakes with External Boundary Layer, without Boundary-Layer Bleed.*

2.1. *Significance of Viscous Interaction.*

Some typical situations are depicted in Fig. 1. The diagrams indicate the basic flow environments, ignoring the way in which the patterns may be changed by viscous interation.

It is seen that essential conditions in the pre-entry flow consist of the following:

(a) in subsonic flow, a boundary layer in a region of pre-entry compression; and,

(b) in supersonic flow, a boundary layer in conjunction with a normal shock, possibly also followed by subsonic pre-entry compression.

Basically both these conditions can be simulated using a pitot-type intake on a flat plate, which was the arrangement employed in the present tests.

The significance of viscous interaction in these situations can be judged by reference to some results given[1,2] by W. F. Davis and others (NASA, Ames, 1948) from a research model of side intakes enclosing various proportions of the body circumference, tested at low supersonic speeds. Losses of total pressure from friction and from the normal shock, according to flow patterns of the type indicated in Fig. 1, can be estimated and the deduced pressure recoveries compared with the measured results. The comparisons are shown in the Table below:

TABLE 1

Comparison of Side Intake Pressure Recoveries with Estimates Neglecting Viscous Interaction ($M_\infty = 1{\cdot}4$)

Percentage enclosed by intake	37%	61%	100%
Estimated loss at full mass flow ($\%P_\infty$)			
(a) Friction (ext.+int.)	5	7	9
(b) Shock wave	4	4	4
Total	9	11	13
Deduced pressure recovery ($\%P_\infty$)	91	89	87
Measured pressure recovery ($\%P_\infty$)	79	75	65

It is seen that the losses from viscous interaction, represented by the difference between deduced and measured pressure recoveries, and here considerably larger than the known losses from friction and shock wave put together.

As a further example, it is known that conical-centrebody intakes, without bleed, at supersonic speeds exhibit losses additional to the shock and basic frictional losses amounting typically to 5 per cent and in some cases to 10 per cent of total pressure, depending upon Mach number and detail geometry.

2.2 *Pre-entry Separation.*

The nature of the flow as modified by viscous interaction can be deduced from an examination of conditions in the entry plane. Typical Mach number profiles taken across the entry plane normal to the external surface, for a range of mass flow at various free stream Mach numbers, are shown in Fig. 2.

We consider first the results at subsonic speed ($M_\infty = 0{\cdot}51$). At 'full mass flow'

$$(\rho_i V_i/\rho_\infty V_\infty \equiv A_\infty/A_i = 1{\cdot}0),$$

there is no pressure gradient in the pre-entry flow, consequently the profile at entry is, as seen, virtually identical with that of the undisturbed boundary layer on the plate with intake absent. As the flow ratio is reduced the pressure at entry rises (Mach number outside the boundary layer falling) until at a certain value of flow ratio the pre-entry pressure rise is just sufficient to separate the boundary layer. Below this value the flow is as shown in the illustrative sketch. The pressure in the entry plane now remains constant at the value corresponding to separation; this is shown by the constant Mach number outside the viscous layer. Reduction of mass flow is now achieved by the separation point moving progressively upstream from the entry plane, thereby increasing the height of the deadwater region at the base of the entry, as revealed by the profiles.

At supersonic speed ($M_\infty = 1{\cdot}20$) the picture is basically similar. An essential difference is that at full mass flow a normal shock sits across the entry, so that the Mach profile immediately behind it shows the corresponding reduction to subsonic speed. However at the particular Mach number of the illustration the normal shock is of itself not sufficient to separate the boundary layer, hence some reduction of mass flow is possible before separation occurs. The process then follows essentially similar lines to that at subsonic speed. After separation, the shock is bifurcated as shown in the illustration. Again in this regime the Mach number outside the viscous layer remains constant (the static pressure being at the value corresponding to separation) and reduction of flow is produced by upstream movement of the separation point.

It may be noted that the end point in this process, i.e. when the intake flow is reduced to zero, corresponds to the well known flow over a forward facing step, with separation upstream of the step.

The value of flow ratio corresponding on the onset of separation increases with increase of free stream Mach number. Its progression through the speed range from subsonic to supersonic can be seen from a collective plot of static pressure in the entry plane (Fig. 3). At any one Mach number, separation occurs at the point where the static pressure becomes constant. The dotted curve indicates the boundary between unseparated flow (to the right) and separated flow (to the left). It is seen that the range of unseparated flow contracts as Mach number increases and vanishes around $M_\infty = 1{\cdot}3$, at which value the normal shock (as is known from other sources) is itself of just sufficient strength to separate the turbulent boundary layer. For normal shocks above this strength, separation will always occur at the shock unless prevented by special means.

The schlieren photographs at these low supersonic Mach numbers are some-what indistinct, but examples of both separated and unseparated flow can be seen.

2.3. *Overall Effect of Viscous Interaction.*

The progressive tendency to flow separation having been established, we proceed now to consider the effect of such separation on the pressure recovery of an intake.

A separate study has been made[3] of the flow downstream of the interaction of a turbulent boundary layer with a normal shock of strength sufficient to cause separation. It is shown there that following separation the static pressure on the surface remains approximately constant at the separation level for a short distance downstream and thereafter rises towards the value corresponding to non-viscous flow

through the normal shock in the outer stream. This subsequent pressure rise corresponds to a development of turbulent mixing, firstly in the free shear layer bounding the separation bubble and secondly in the rehabilitating boundary layer following reattachment.

A similar flow occurs in an intake following pre-entry separation: in this case the extent of the downstream pressure rise is conditioned by the nature of the diffuser, the flow outside the viscous layer being no longer unbounded.

Fig. 4 shows the pressure development in a typical model of the present series at a Mach number $M_\infty = 1{\cdot}35$ and flow ratio 0·85. The static-pressure rise up to the entry plane is only about one-third of that for non-viscous flow and although a further rise accrues from turbulent mixing as described above, the mixing is of course accompanied by a loss of total pressure; so that at the end of the diffuser both static and total pressure lie well below the values which would correspond to a flow with normal shock and wall friction but without viscous interaction.

Thus the effect of the viscous interaction is to set up a zone of turbulent mixing in which a loss of total pressure occurs and this is reflected in the final pressure recovery of the intake. It may be noted that even in cases where the pre-entry pressure rise is insufficient to cause actual separation, it may nevertheless cause distortion of the boundary layer profile and hence turbulent mixing in the subsequent rehabilitation, leading to significant though smaller loss in total pressure. The point is of some importance to the subsonic design problem; since although, as we have seen, it is possible to design for no pre-entry separation, some loss of pressure recovery from the viscous interaction may nevertheless be inevitable.

The possible order of magnitude of loss from viscous interaction and the way in which it develops through the transonic speed range are illustrated in Fig. 5, which shows results for a particular model of the series, tested through the Mach range 0·5 to 1·8. Peak pressure recovery at each Mach number is plotted and compared with the estimated losses from friction and the normal shock. A particular form of pressure recovery (sometimes called the 'ram efficieny') is used which enables results for incompressible flow, estimated according to Ref. 4, to be included for comparison. It must be noted that the abcissa of the graph corresponds not to a scale of flight speed but to a scale of design Mach numbers, the flow in the intake being at all points that corresponding to a high-speed condition (i.e. flow ratio $\leqslant 1{\cdot}0$).

The following conclusions are to be drawn:

(1) At speeds up to about Mach 0·5, frictional losses consitute in effect the whole total-pressure loss.

(2) Loss from viscous interaction is significant at high subsonic speeds, amounting to perhaps 25 per cent of the total loss.

(3) Above $M = 1$, the loss from viscous interaction develops rapidly and up to $M = 1{\cdot}6$ or so is the major component of loss.

This result is significant not only for pitot-type side intakes at low supersonic speeds but also in general for supersonic intakes with external-compression surfaces, since the Mach number of the terminal shock is normally within this range.

(4) At higher speeds than $M = 1{\cdot}6$, the shock loss itself dominates but the interaction loss is still potentially very significant, amounting at $M = 1{\cdot}8$, in the case shown, to 15 per cent on ram efficieny which is equivalent to 10 per cent on total-pressure ratio.

3. *Quantitative Assessment.*

3.1. *Experimental Details.*

For a quantitative assessment of interaction loss, measurements have been made of the pressure recovery of a variety of intake shapes with various boundary-layer conditions. Interaction loss was deduced by comparing the measured losses with the calculated friction and shock losses.

The experimental arrangement is depicted in Fig. 6 and Fig. 7 shows the range of intake shapes. The thickness of the external boundary layer—always turbulent—was also varied, by changing either the position of the model on the plate or the calibre of the roughness strip used to produce transition.

Each intake was tested over a range of mass flow and in general at each of the following Mach numbers:

M_∞ = 0·72, 0·95, 1·05, 1·20, 1·35, 1·52 and 1·83. In all over one hundred separate characteristic curves of pressure recovery *versus* mass flow were established.

3.2. *Significance of Boundary-Layer Capture Ratio.*

The main body of experiments was concerned with the effect of varying the boundary-layer capture ratio at each Mach number. For these tests the area ratio and area distribution of the internal diffuser were kept constant.

Boundary-layer capture ratio is defined as

$$A_\theta/A_i = (\theta \times w)/A_i\,,$$

where A_i is the entry area,

w is the entry width at the surface

θ is the momentum thickness of the undisturbed boundary layer at the position of the entry with intake removed.

Typical results are shown in Fig. 8. Apart from reaffirming the large magnitude of interaction loss particularly at low supersonic speeds—model Z is identical with model B except for the absence of an external boundary layer in the case of Z—the results are significant principally in showing the interaction loss to be a non-linear function of boundary-layer capture ratio at supersonic speeds. Stated more precisely, a linear variation exists over the range of A_θ/A_i covered in the tests but if this variation is extrapolated back to zero A_θ/A_i, a significant discrepancy remains between the result so obtained (dotted curve in Fig. 8) and that for the true pitot intake, model Z.

This effect, which is confirmed throughout the whole set of experiments, is the result of a dual nature in the boundary-layer interaction. Where, on the one hand, the interaction involves a distributed pressure gradient as in subsonic forespillage (at both subsonic and supersonic speeds) and again in the internal diffuser, the gradient being determined by intake geometry or mass-flow ratio, independently of the boundary-layer thickness, then a natural result is that the scale of the interaction loss should vary with the degree of boundary-layer capture. Essentially this is the linear variation shown by the results. On the other hand, where the interaction is *via* a shock wave, the pressure gradient is governed by the boundary-layer thickness itself, in such a manner that the thinner the boundary layer, the sharper is the pressure gradient*. Consequently the quantitative effect of that part of the interaction which is produced directly by the shock wave tends to be independent of the boundary-layer thickness. Essentially this is the residual loss shown in Fig. 8 as between the pitot intake, model Z, and the extrapolated result for zero, or more correctly, indefinitely small, boundary-layer capture ratio.

A practical approach is therefore to regard the total interaction loss as being the sum of two components:

(1) a boundary-layer component, proportional to the capture ratio A_θ/A_i and existing at both subsonic and supersonic speeds; and

(2) a shock-wave component, independent of capture ratio and existing only at supersonic speeds.

It is of course questionable whether this analysis would hold at very small values of the capture ratio, for which some decrease in magnitude of the shock component might be expected. However the full range of present experiments failed to reveal any such tendency, and it is suggested that this form of analysis is certainly valid for values of A_θ/A_i greater than 0·005. This is the basis of an emperical generalisation of interaction loss which now follows.

---

*This results, for example, in the pressure rise to separation at a shock being independent of boundary-layer thickness. Otherwise put, a normal shock at Mach 1·3 (approximately) will just cause separation of a turbulent boundary layer, however thin.

3.3. *Generalisation of Interaction Loss.*

The previous discussion leads to a suggestion that the interaction loss can be represented generally in the form

$$\Phi \frac{A_\theta}{A_i} + \Psi ,$$

where Φ and Ψ are functions of Mach number, possible unique. Before this can be established, however, it is necessary to take out a variation with mass flow at any Mach number.

Using the argument that for an intake in incompressible flow, the overall pressure rise, including that in the internal diffuser, is proportional to $[1-(A_\infty/A_m)^2]$ the trends of interaction loss with flow ratio were examined in terms of $[1-(A_\infty/A_m)^n]$ on the grounds that a modified power would be required for compressible flow. It was found that for each intake at any Mach number, subsonic or supersonic, the interaction loss could with sufficient accuracy be taken to be proportional to the mass flow function:

$$Q \equiv 1-(A_\infty/A_m)^3 . \tag{1}$$

The correlations at $M = 1{\cdot}83$ are shown in Fig. 9. The theoretical maximum flow at supersonic speeds being $A_\infty/A_i = 1{\cdot}0$, the maximum value of $(A_\infty/A_m)^3$ for any intake is

$$(A_\infty/A_m)^3 \text{ max} = (A_i/A_m)^3$$

i.e. the cube of the inverse diffuser area ratio. For most intakes this has a relatively small value. Only in the case of model N (a parallel duct) could the value

$$A_\infty/A_m = 1{\cdot}0$$

be approached, but the result for this model (repeated at other Mach numbers) gives convincing evidence for the assumption that interaction loss should tend to zero as that value is approached*. The pressure recovery of model N, with $A_\infty/A_m = 1{\cdot}0$, through the Mach number range, is shown additionally in Fig. 8, confirming the absence of any significant interaction loss in this case.

A mass flow dependence having been established, it is now possible from each measured pressure-recovery characteristic to derive a value of $\Delta P_i/P_\infty Q$, where ΔP_i is the interaction loss. The values for different intakes, boundary-layer conditions and Mach numbers can then be correlated in such a way as to establish values for the Mach-number functions in the generalised form.

Models additional to the main series were included to cover changes in area ratio (models L, M, N) and in area distribution (models P, Q, R, S) of the internal diffuser. It was found possible to bring these cases within the scope of the generalisation by developing the factor multiplying the boundary-layer function so as to include, in addition to the capture ratio A_θ/A_i, the diffuser area ratio A_m/A_i and a shape parameter A_h/A_i. For this last, A_h was taken quite arbitrarily to be the area half-way along the diffuser, this giving a simple indication of relative rates of diffusion in the initial and final parts of the diffuser. No great generality would be claimed for this part of the analysis without a more extensive experimental investigation.

As a result of the analysis now described, the interaction loss is expressed finally in the following general terms:

$$\frac{\Delta P_i}{P_\infty} = Q(K\Phi + \Psi), \tag{2}$$

where Q is the mass flow function defined above,

---

*This is saying that with no subsonic pressure rise either in the diffuser or in the pre-entry flow, the interaction loss is negligibly small.

$$K \equiv \frac{A_\theta}{A_i}\frac{A_i}{A_m}\left[0{\cdot}6+2{\cdot}4\left(\frac{A_h}{A_i}-1\right)\right], \tag{3}$$

$\Phi \equiv \Phi(M)$ is the boundary-layer function,

$\Psi \equiv \Psi(M)$ is the shock function.

A numerical multiplier in the expression for K could alternatively be absorbed into the function Φ. The particular factor used is chosen such that for the main series of models, with $A_m/A_i = 1{\cdot}5$ and $A_h/A_i = 1{\cdot}375$, the expression for K reduces simply to

$$K = A_\theta/A_i\,. \tag{4}$$

The final correlations leading to determination of the Mach functions Φ and Ψ are shown in Fig. 10. The functions themselves are plotted in Fig. 11. In Fig. 12 curves of $\Delta P_i/P_\infty Q$ are plotted for different values of K. With the help of the inset diagram, giving the evaluation of Q from the flow ratio A_∞/A_i, the chart may be used for rapid calculation of the interaction loss in any given case.

4. *General Discussion.*

A description has been given of the nature of flow in any air intake in which an external boundary layer is subjected to an adverse pressure gradient in the pre-entry region including the effect associated with the normal shock (if any). A formula has been proposed for calculating, in the absence of boundary-layer bleeds or equivalent devices, the effect of the interaction on pressure recovery of the intake. Whether the external boundary layer is a consequence of the particular location of an intake in an aircraft (e.g. fuselage boundary layer with a side intake) or is that developed on a component of the intake itself (e.g. the external-compression surface of a supersonic intake), the approach is essentially and within limits the same.

4.1. *Limitations.*

The principal limitations in application of the general formula are as follows:

(1) In all the experiments the length of internal diffuser was constant and equal to 7·5 times the hydraulic diameter* of the measuring section. For practical application of the formula in cases where the diffuser length is significantly greater than this, it is suggested that a section in the duct should be determined for which the length is as stated; this station then to be used as the effective A_m. If significantly shorter diffusers are involved, adaptation of the formula is less obvious; however it may be noted that in all the diffusers tested, the final 2·5 diameters was at constant area. No great error is likely, therefore, if the formula is applied for diffusers down to 5 hydraulic diameters in length.

(2) The investigation of changes in diffuser shape was strictly limited in extent and this part of the generalised result carries less confidence than that describing the basic effect of boundary-layer capture. The implication is that estimates by the formula may become increasingly inaccurate as conditions depart the further from those of the main series of tests ($A_m/A_i = 1{\cdot}5$, $A_h/A_i = 1{\cdot}375$).

(3) Curvature of the duct, particularly near the entry, can have an important effect. The fact that this has not come within the scope of the present investigation represents the most significant limitation in connection with applying the general results to intakes with cone or wedge centrebodies, where the throat region of the duct is almost always curved. Particular investigations of curvature effects have been made e.g. Ref. 5 and the most useful next stage in a continuation of the general study would be to link these investigations into the present approach.

---

*Hydraulic diameter is defined as twice the cross-sectional area divided by the perimeter length.

4.2. *Independent Checks.*

The interaction loss formula has been independently checked at high Reynolds number by means of free-flight tests of a side intake model, the intake being semi-elliptic in shape alongside a cylindrical fuselage with ogival nose. Two models were flown of identical design but with different mass flows.

Model and results are shown in Fig. 13. It is seen that the deficiency of pressure recovery as compared with normal shock is well predicted by the general formula.

Checks have also been made of the applicability of the formula to cases of conical and wedge centre-body intakes for which wind tunnel results are available. Generally, the formula gives a reasonable first approach to the interaction loss in these cases, the chief limitation being a lack of allowance for the effect of duct curvature—*see* Section 4.1.

4.3. *Boundary-Layer Bleeds.*

A boundary-layer bleed, if properly designed, is usually capable of reducing the interaction loss effectively to zero. If a bleed is to be employed, a contribution of the present study is that it provides a means of assessing bleed efficiency, which can be useful. The purpose of the bleed being primarily to eliminate the interaction loss and to remove external boundary layer, its efficiency is defined as:

$$\eta_{\text{bleed}}(\%) = 100 \times \frac{\left[\dfrac{P_m}{P_{\infty(\text{measured})}} - \dfrac{P_m}{P_\infty}(\text{calc. for no bleed})\right]}{[\text{Ext. friction loss} + \text{Interaction loss}]}$$

and this can be calculated, using the interaction-loss formula of equation (2).

A comparison of efficiencies of particular flush and pitot-type bleeds (Fig. 14) shows that both can be reasonably efficient over a wide range of local Mach number. Flush bleeds are usually preferred for the throat position in supersonic intakes, where the local Mach number is low-supersonic and where pitot-type bleeds can produce undesirable choking effects.

A bleed should preferably be positioned at or just downstream of the normal shock position. Interaction of the shock with a new boundary layer behind the bleed is thereby avoided. The design of a supersonic intake with internal compression may require the normal shock to be downstream of the bleed for other reasons: in this case the shock should be stabilised at the downstream lip, where the boundary-layer thickness is effectively zero i.e. $A_\theta/A_i \ll 0{\cdot}005$.

It has been shown that the interaction loss is much more severe at supersonic than at subsonic speeds. In this respect therefore the fuselage bleed or diverter of a side intake is less important below $M = 1$ than above, and where the emphasis is on subsonic cruise efficiency a saving in bleed drag may be vital. Some systematic work on the rate of degradation of bleed (or diverter) efficiency at supersonic speeds with reduction in subsonic drag would be useful.

4.4. *Area Ratio and Shape of Internal Diffuser.*

The area ratio A_m/A_i has an important bearing on the level of interaction loss at supersonic speeds. Unfortunately this ratio tends to be confined within narrow limits by, on the one hand, the need to keep the terminal shock loss low and on the other the level of velocity prescribed for entry to the engine. Thus in round numbers, if the terminal shock Mach number is 1·3, giving Mach number 0·8 after the shock, and the Mach number at entry to the engine is 0·4, the required diffuser area ratio is 1·5. For critical flow in the intake, the mass-flow factor Q in equation (2) has then a value 0·7. To reduce this by half would involve reducing the diffuser area ratio to 1·15, which for the same Mach number at engine face, would require the normal shock to be at a Mach number around 2·5, a quite impracticable concept.

The shape parameter A_h/A_i lends itself more readily to variation, given adequate length in the duct. Equation (2) shows that, with area ratio 1·5, a change from a linear diffuser ($A_h/A_i = 1{\cdot}25$) to one which the area is constant up to the halfway station ($A_h/A_i = 1{\cdot}0$) will halve the value of the boundary-layer loss term.

4.5. *Vortex Generators.*

In the case of side intakes with a fairly long external boundary layer, it is possible that vortex generators can be used to inhibit flow separation and thereby reduce the interaction loss. The result of a test on the flat plate is shown in Fig. 15. It is seen that separation has been avoided and the static pressure rise thereby considerably accelerated.

The result for a flush boundary-layer bleed is included in Fig. 15 for comparison. The pressure rise with bleed approaches closely to the theoretical value for no interaction. Clearly as far as internal flow is concerned a bleed is the best solution to the problem of interaction loss. However if other solutions are to be sought in the interests of subsonic drag, a possible approach would seem to be to use vortex generators to inhibit separation, in combination with a low initial expansion rate in the internal diffuser.

5. *Conclusions.*

(1) The nature of the flow in intakes with external boundary layer, at subsonic and supersonic speeds, has been described. It is shown how, in the absence of boundary-layer control, the interaction between the boundary layer and the pre-entry pressure gradients, including where present the normal shock, can dominate the flow and ultimate pressure recovery, particularly for low supersonic speeds ahead of the normal shock.

(2) From the results of wind-tunnel experiments with a variety of intake shapes, an empirical formula is derived expressing the interaction loss in general terms. The loss is shown to be expressible as the sum of two components, one depending primarily on the boundary-layer capture ratio and present at both subsonic and supersonic speeds, the other present at supersonic speeds only, resulting from the special nature of shock wave and boundary-layer interaction. The results of independent checks of the formula are shown.

(3) The problems of boundary-layer control are discussed briefly, with particular reference to the case where it is necessary to combine adequate intake performance at supersonic speeds with minimum drag at high subsonic speed. It is suggested that work of a special kind on bleeds and diverters is required. Alternatively the use of vortex generators in combination with a low initial rate of diffusion in the duct may be tried.

LIST OF SYMBOLS

ρ	Density
V	Velocity
M	Mach number
p	Static pressure
P	Total pressure
A	Cross-sectional area
w	Width of entry across and coincident with the external surface
l	Length of internal diffuser, from entry to measuring section
θ	Momentum thickness of undisturbed boundary layer at entry position
ΔP_i	Interaction loss i.e. loss of total pressure caused by interaction of boundary layer and adverse pressure gradients
Q	Mass-flow function, $1-(A_\infty/A_m)^3$
Φ, Ψ	Mach number functions in expression for interaction loss
K	Boundary-layer parameter in expression for interaction loss
η_R	Ram efficiency of an intake $= (P_m-p_\infty)/(P_\infty-p_\infty)$
η_{bleed}	Efficiency of boundary-layer bleed

A.B.C.D.E.; L.M.N.; P.Q.R.S.; Z are reference lettes for model intake shapes of the systematic series

Suffices:

∞	Denotes free stream conditions
i	Denotes entry plane
m	Denotes measuring section
h	Denotes section of diffuser halfway (in distance) between entry and measuring section

REFERENCES

No.	*Author(s)*	*Title, etc.*
1	W. F. Davis D. L. Goldstein	Experimental investigation at supersonic speeds of twin-scoop duct inlets of equal area. I An inlet enclosing 61 % of the maximum circumference of the forebody. N.A.C.A. R.M. No. A7J27, January 1948.
2	W. F. Davis S. S. Edwards	Experimental investigation at supersonic speeds of twin scoop inlets of equal area. III Inlet enclosing 37·2 % of the maximum circumference of the forebody. N.A.C.A. R.M. No. A8E04, July 1948.
3	J. Seddon	The flow produced by interaction of a turbulent boundary layer with a normal shock wave of strength sufficient to cause separation. A.R.C. R. & M. 3502, March 1960.
4	J. Seddon	Air intakes for aircraft gas turbines. J. R. aero. Soc. October 1952, pp. 747–781.
5	E. L. Goldsmith	The effect of internal contraction, initial rate of subsonic diffusion and cowl and centrebody shape on the pressure recovery of a conical centrebody intake at supersonic speeds. A.R.C. R. & M. No. 3204, November 1956.

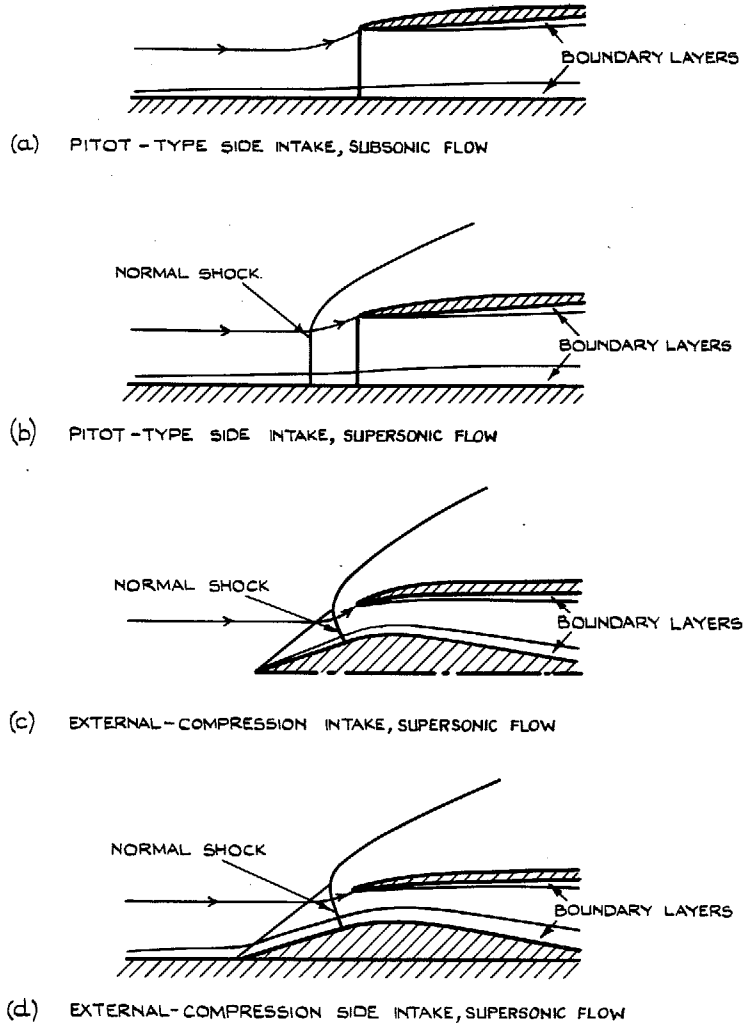

FIG. 1. Intakes with external boundary layer.

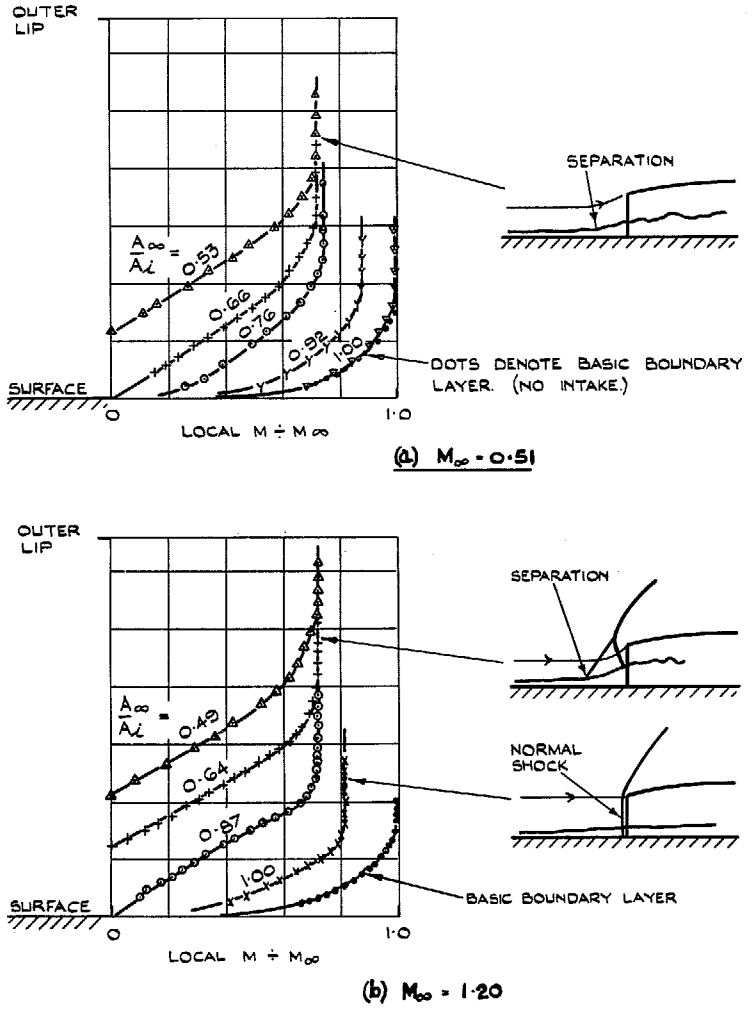

FIG. 2. Mach profiles in entry plane.

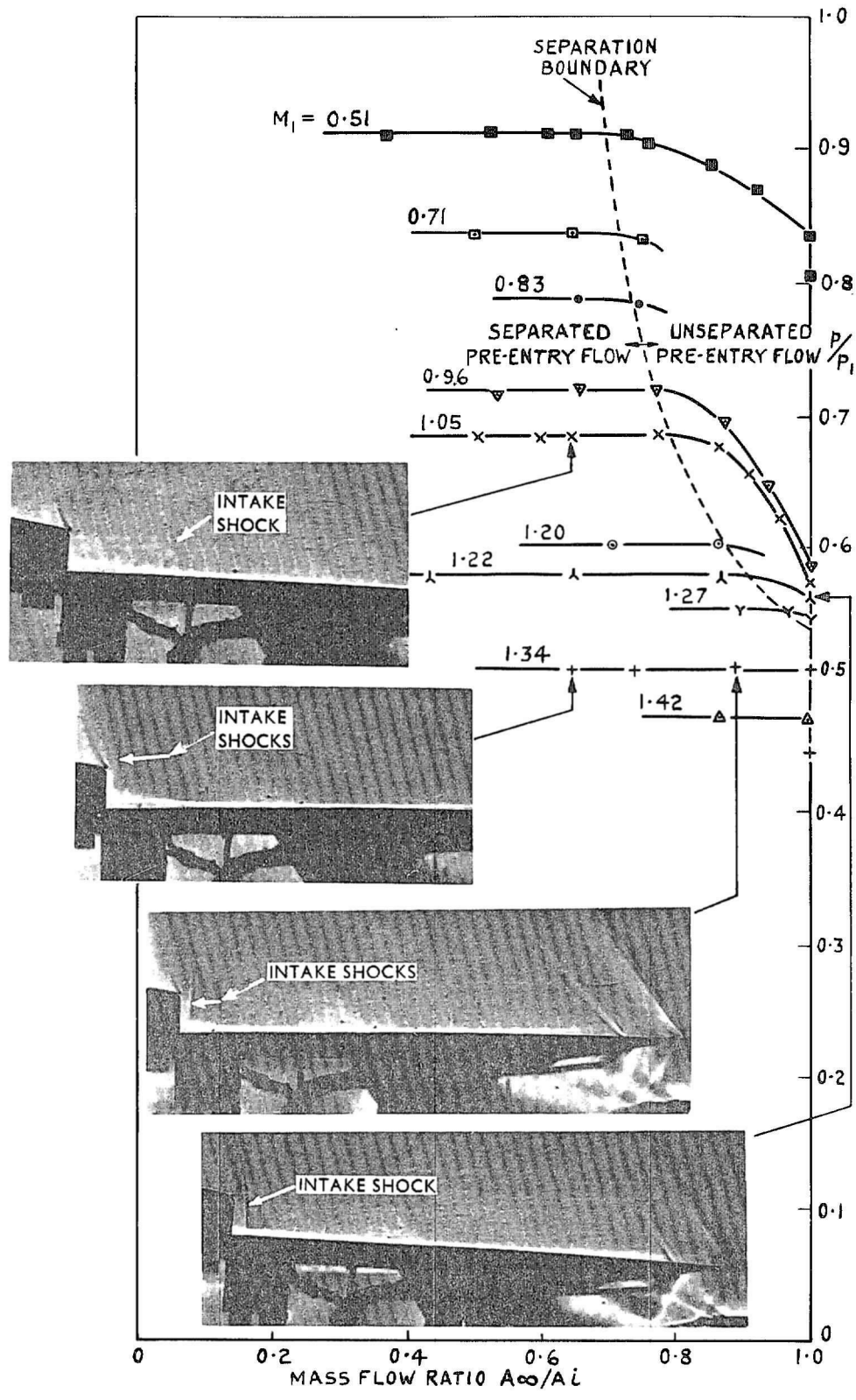

FIG. 3. Progression of flow separation regime through Mach range.

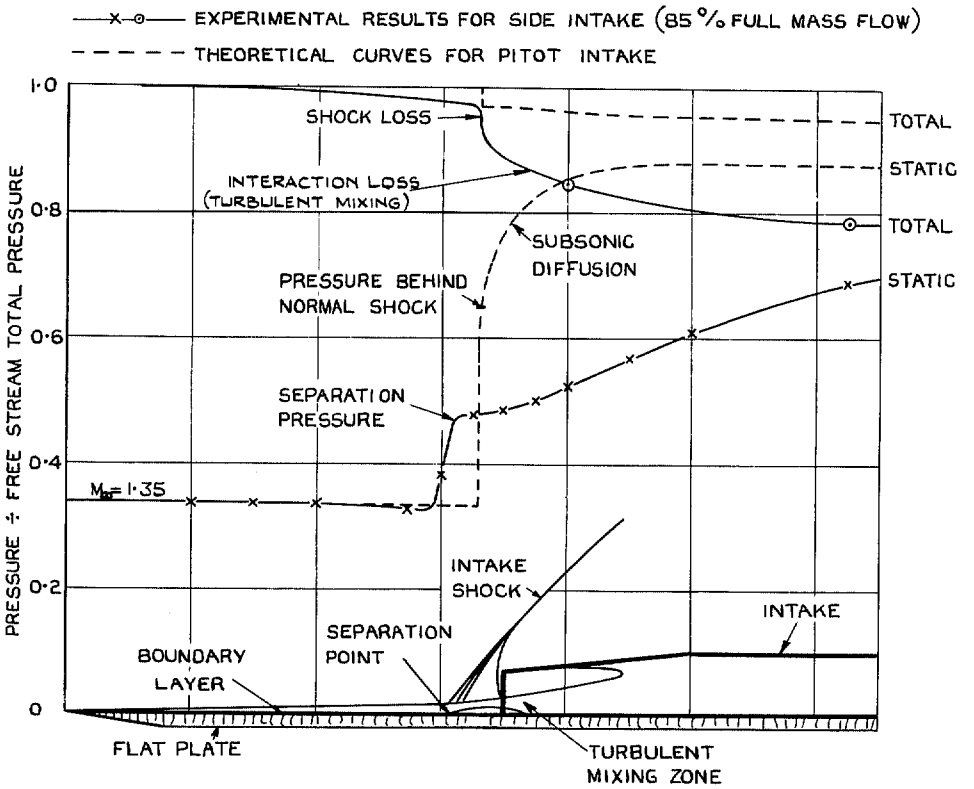

FIG. 4. Flow and pressure recovery in a typical side intake at $M = 1{\cdot}35$.

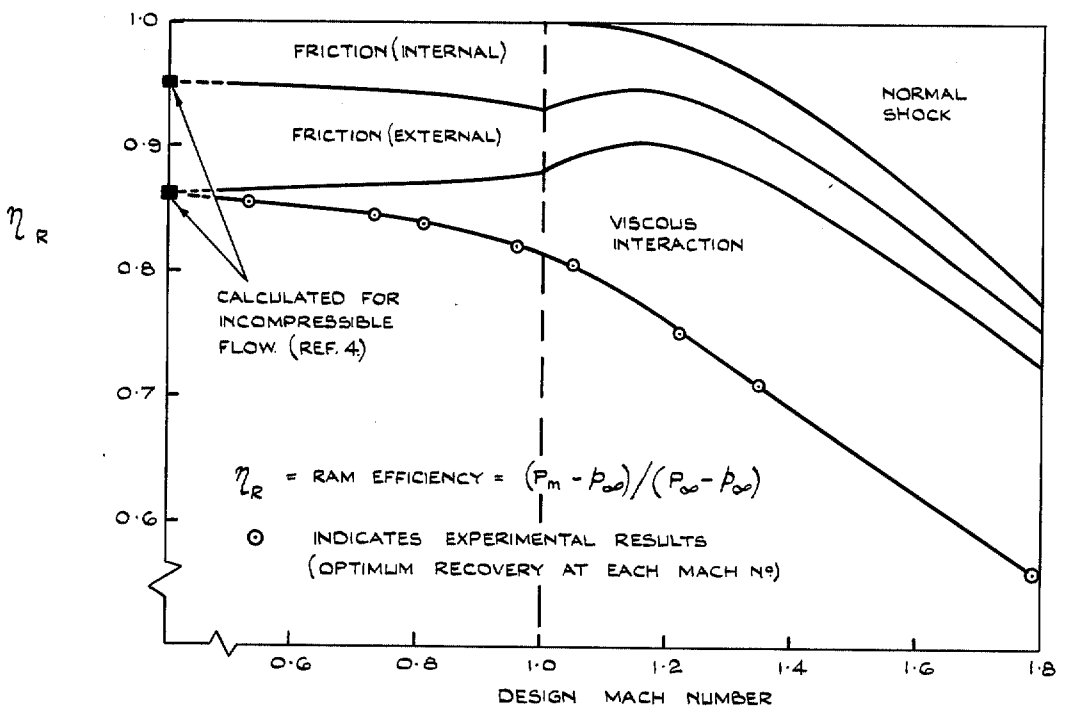

FIG. 5. Analysis of typical side intake results showing relative magnitude of loss from viscous interaction.

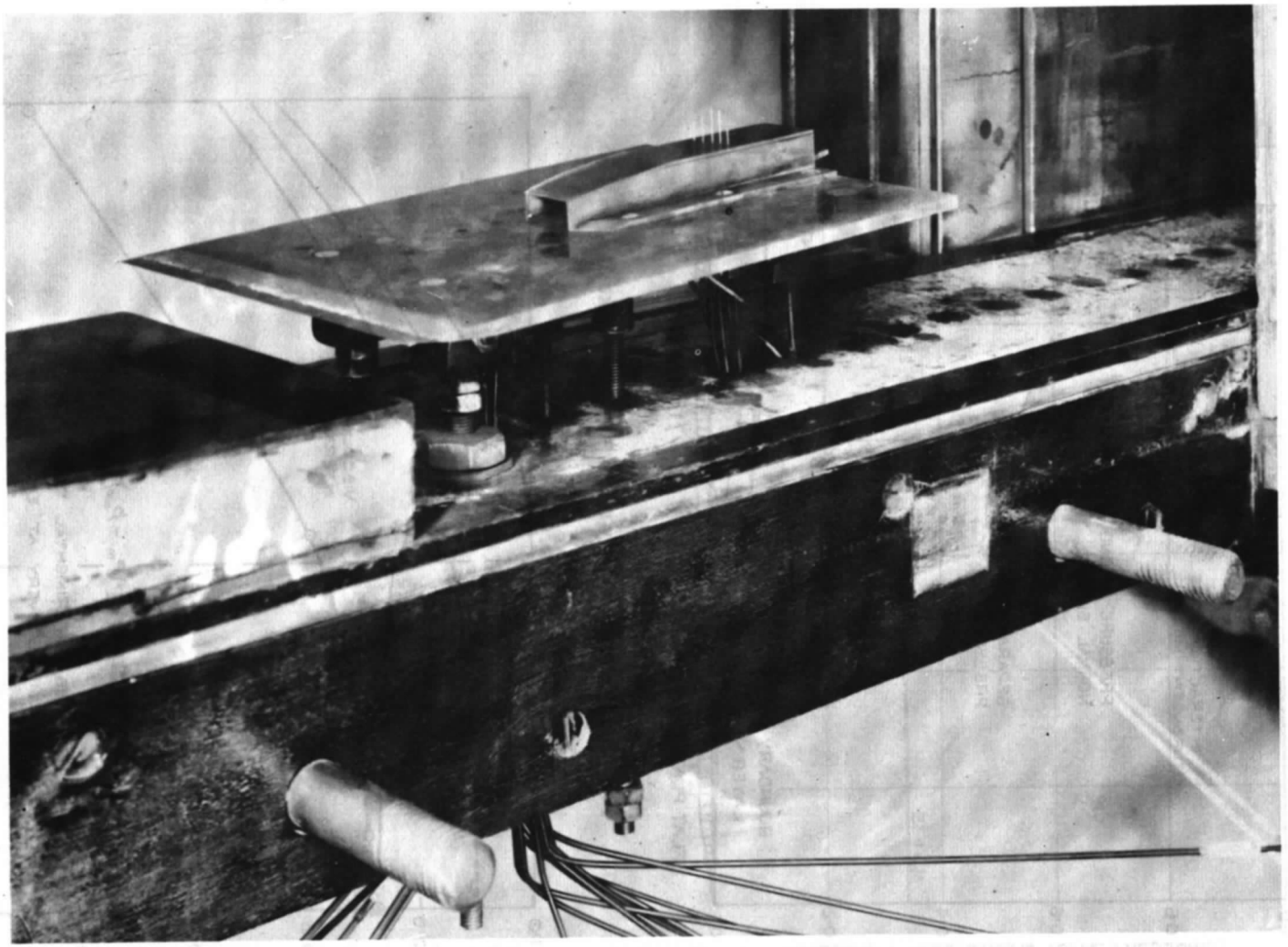

FIG. 6. Experimental arrangement of flat plate model in subsonic/supersonic tunnel (6 in. × 6 in.).

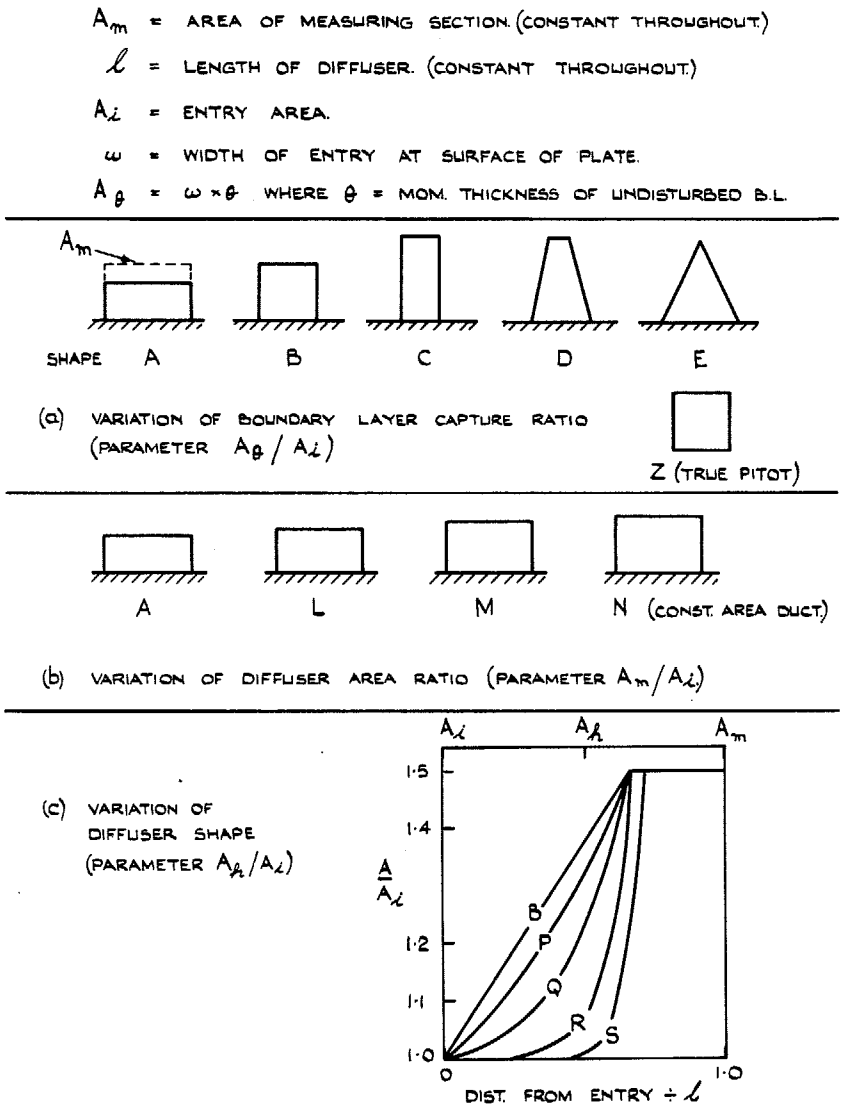

FIG. 7. Range of shapes tested.

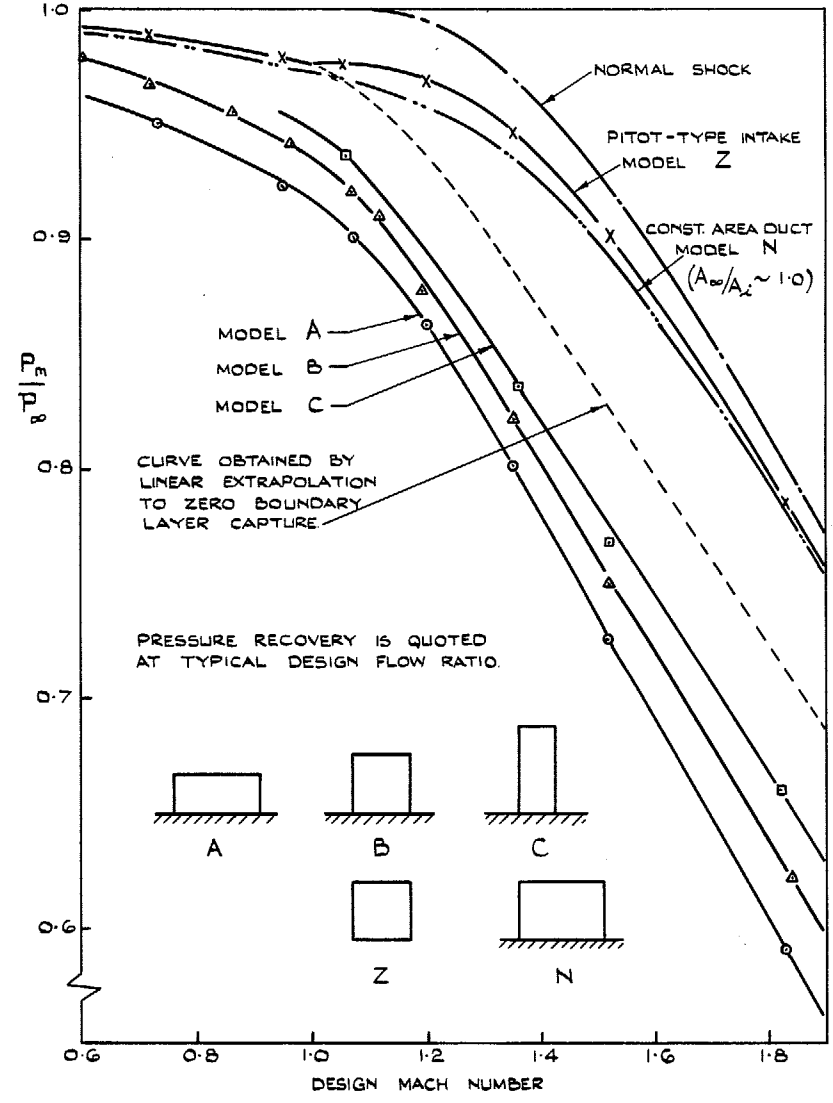

FIG. 8. Typical results showing effect of boundary-layer capture.

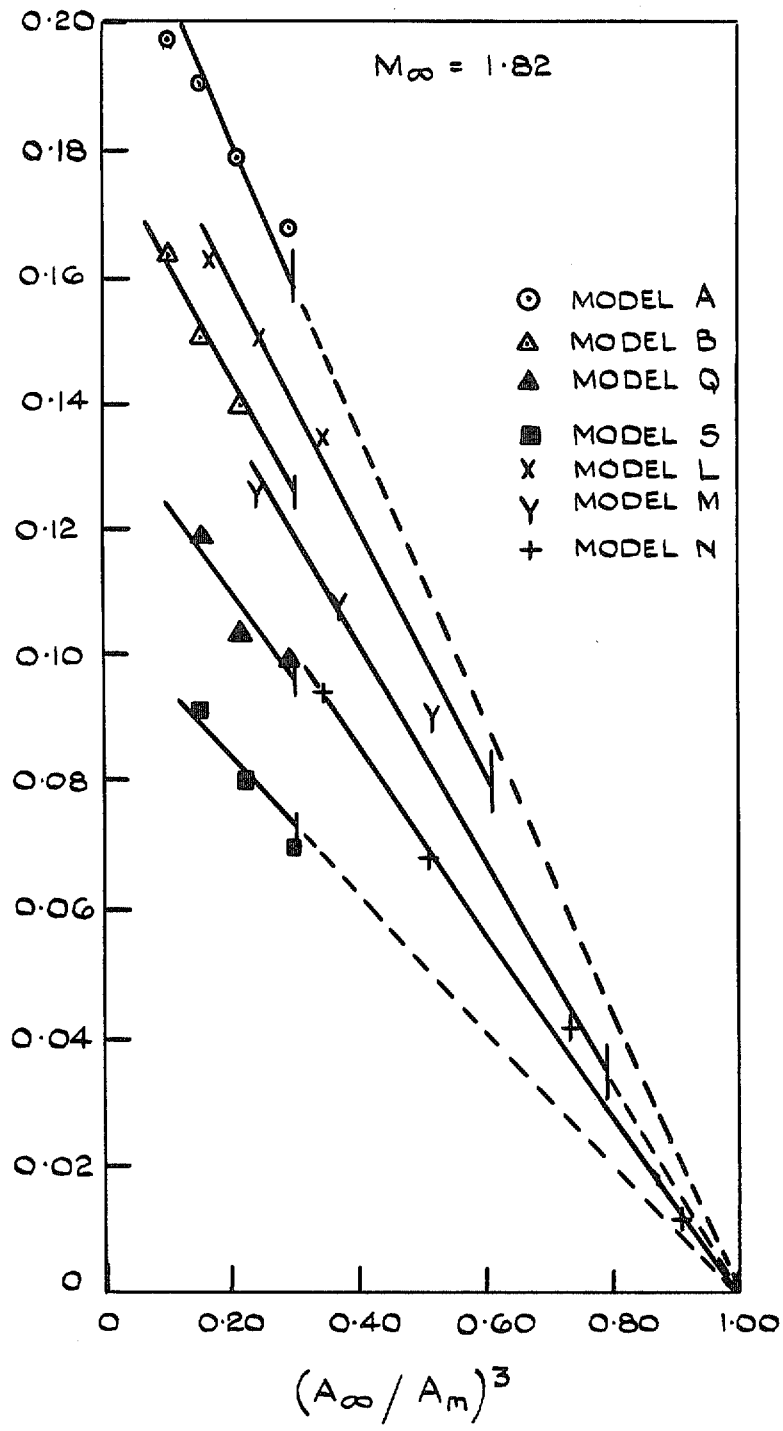

FIG. 9. Interaction loss *vs.* mass flow at one typical Mach number.

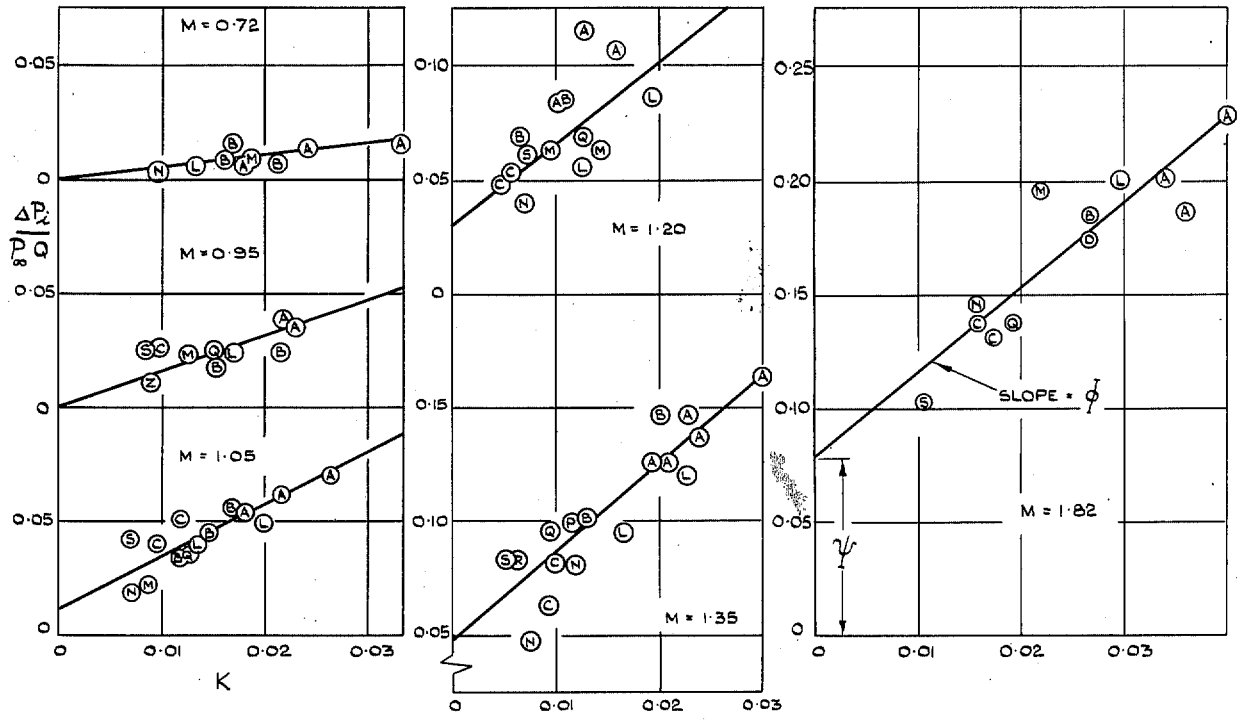

FIG. 10. Correlations for Mach functions Φ and Ψ.

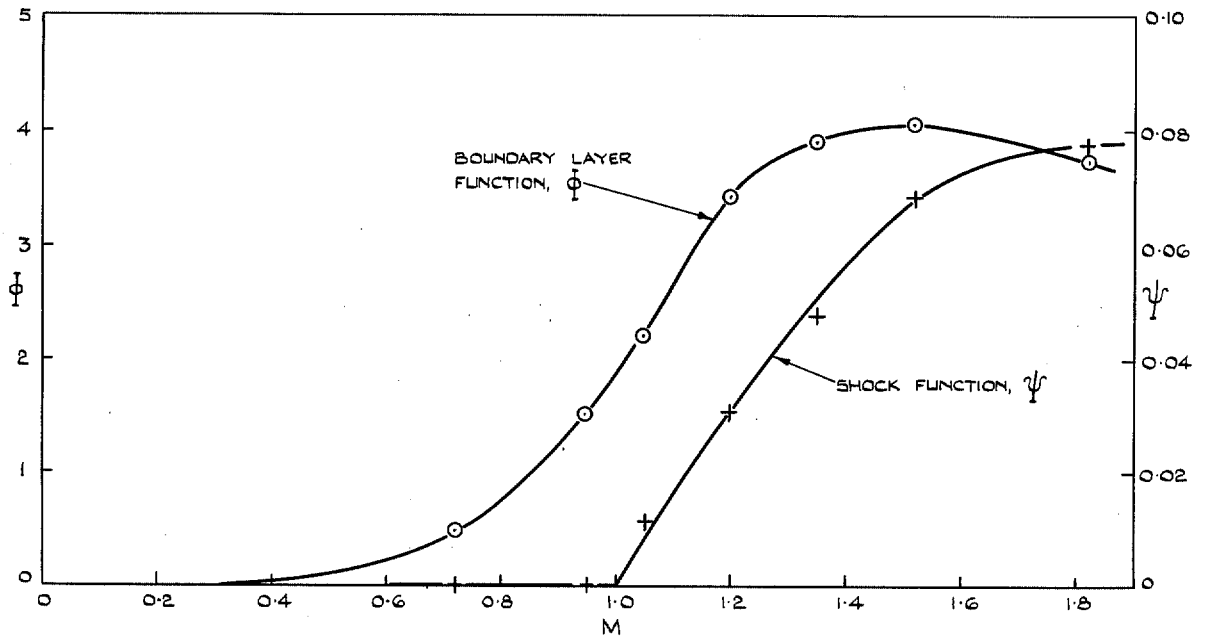

FIG. 11. Mach functions Φ, Ψ determining viscous interaction loss.

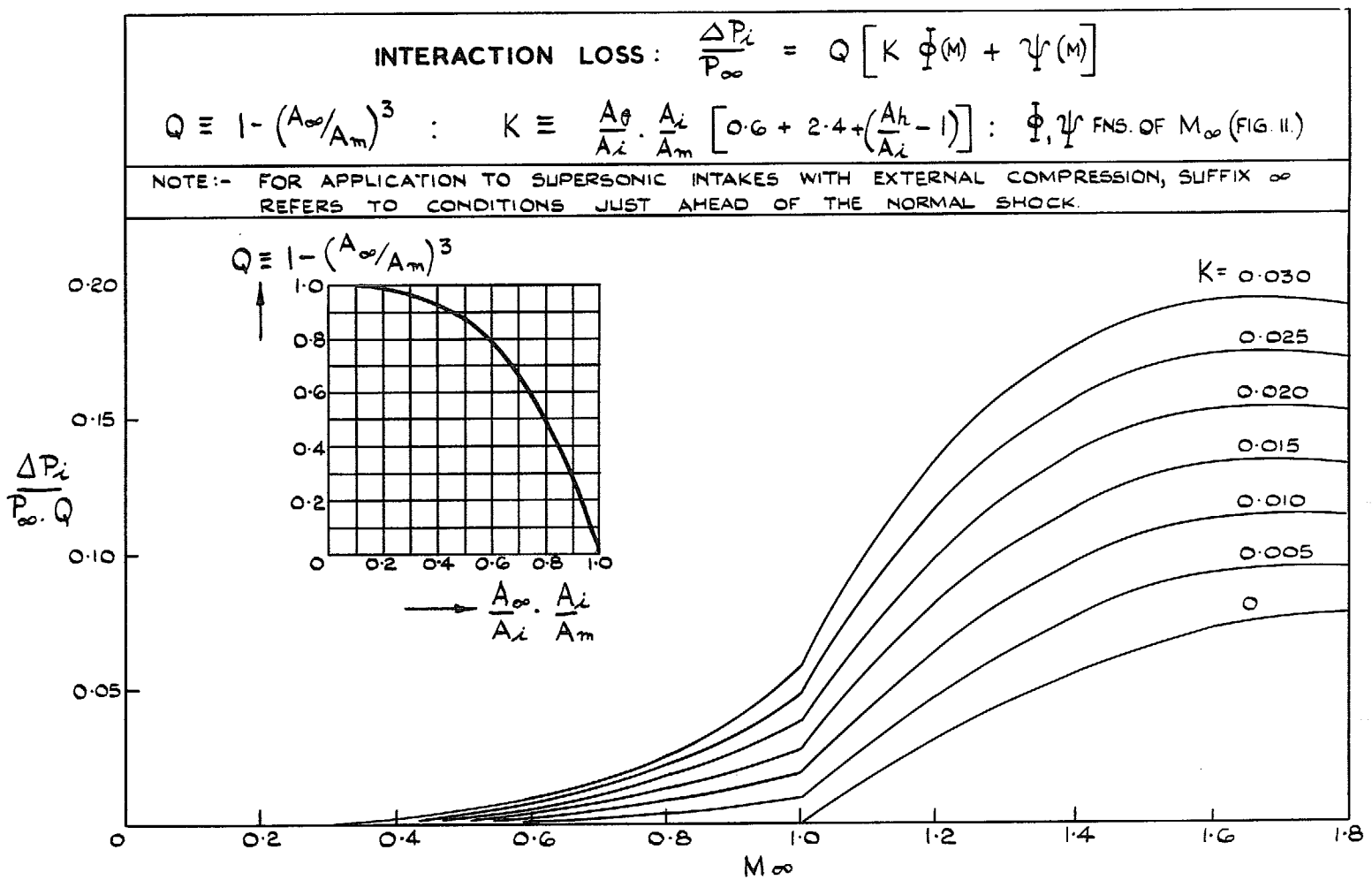

FIG. 12. Generalised results for viscous interaction loss of intakes with external boundary layer.

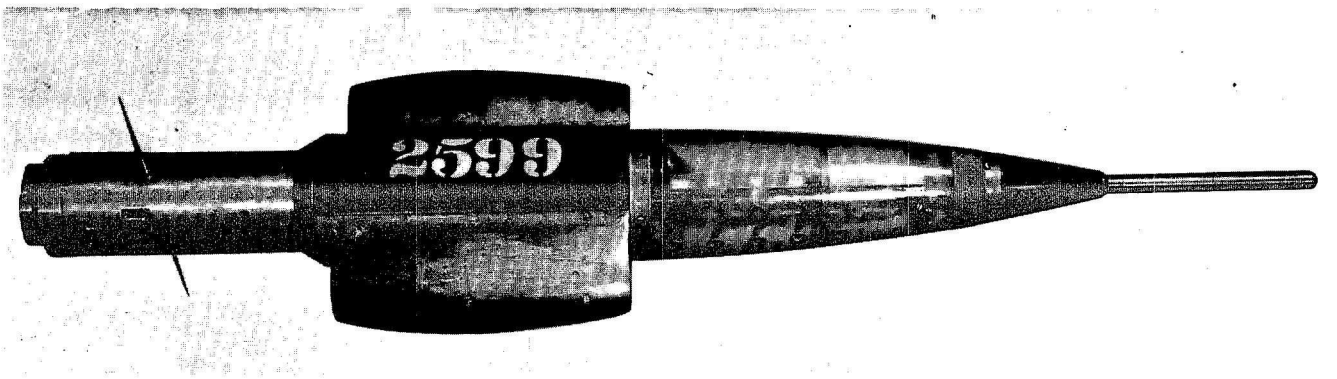

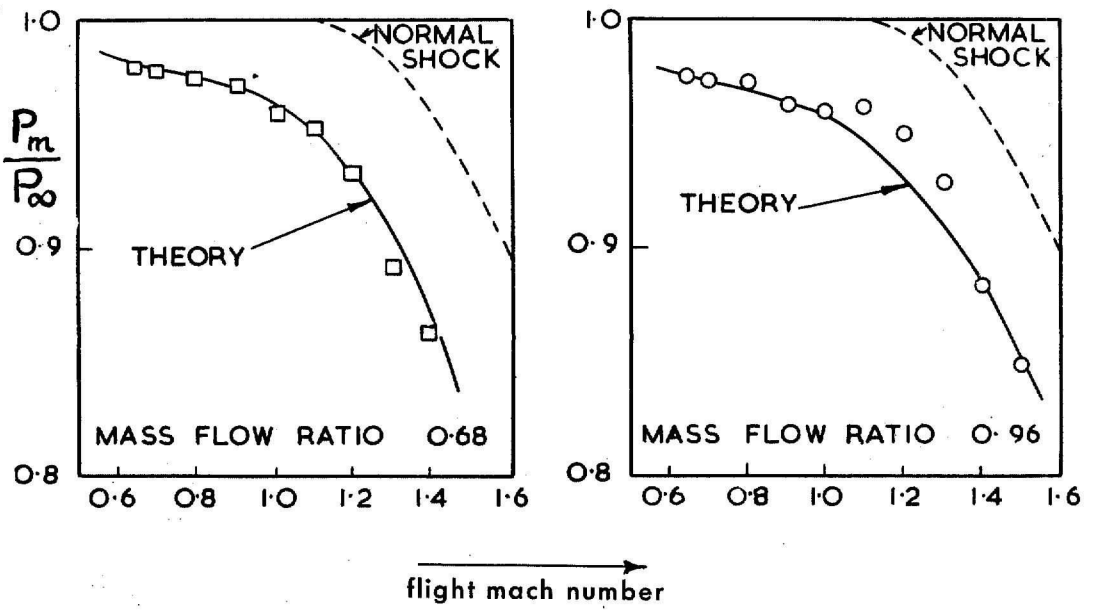

FIG. 13. Results of free-flight test compared with empirical theory.

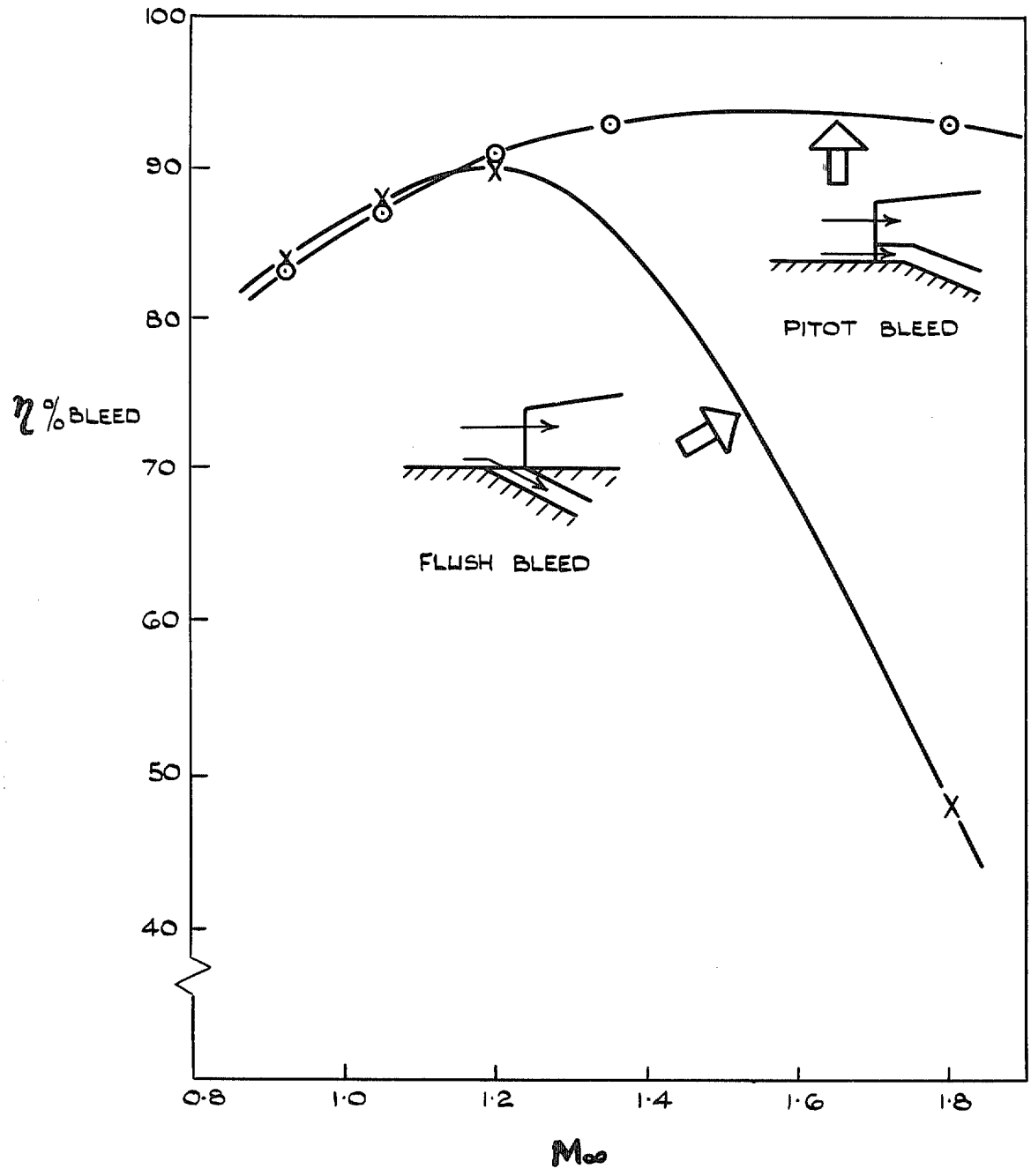

FIG. 14. Efficiency of particular boundary-layer bleeds.

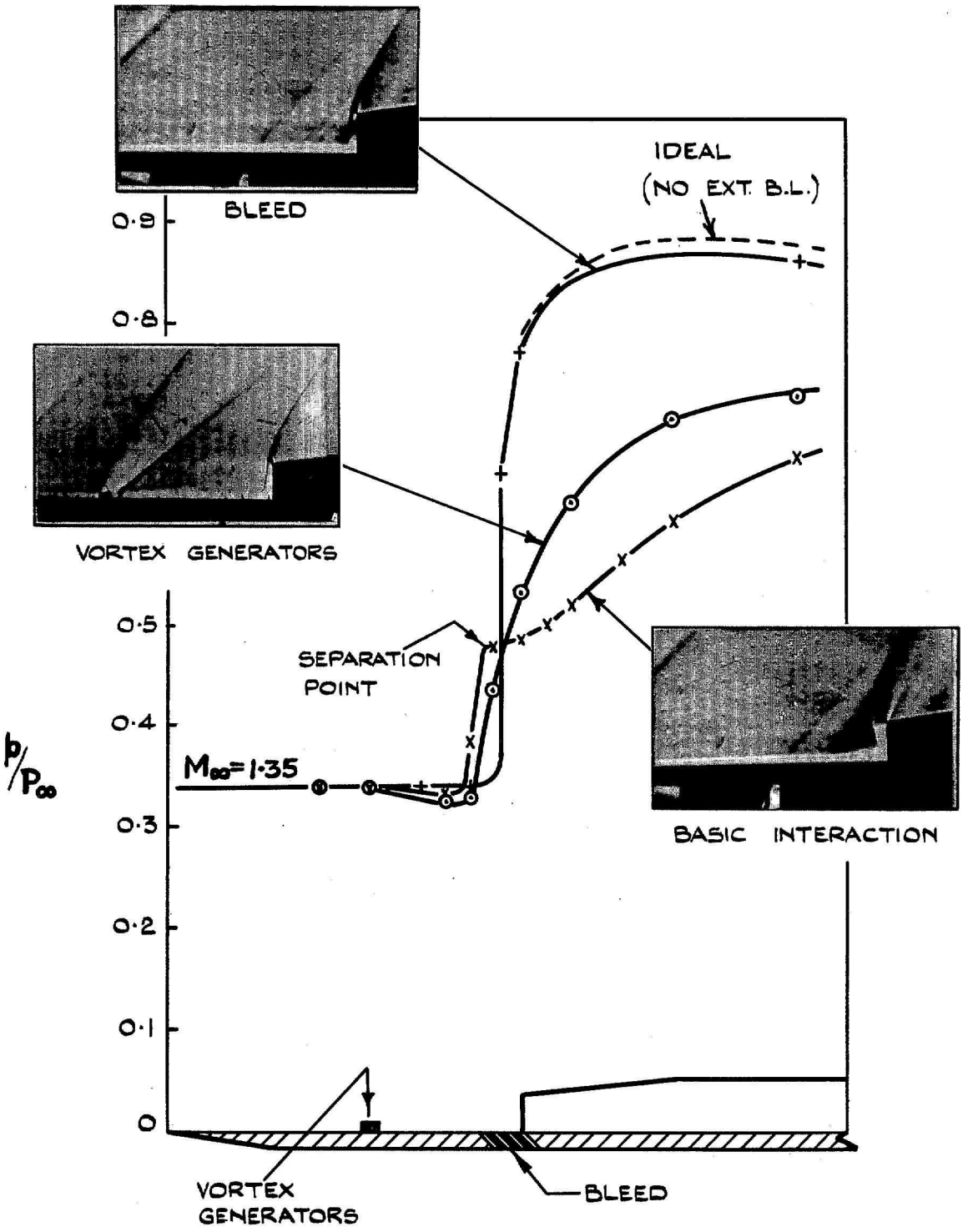

FIG. 15. Typical results with vortex generators or boundary-layer bleed.

Printed in Wales for Her Majesty's Stationery Office by Allens Printers (Wales) Limited.

Dd. 135646 K.5

Published by
HER MAJESTY'S STATIONERY OFFICE

To be purchased from
49 High Holborn, London W.C.1
13a Castle Street, Edinburgh EH2 3AR
109 St. Mary Street, Cardiff CF1 1JW
Brazennose Street, Manchester M60 8AS
50 Fairfax Street, Bristol BS1 3DE
258 Broad Street, Birmingham 1
7 Linenhall Street, Belfast BT2 8AY
or through any bookseller

R. & M. No. 3565

SBN 11 470265 9